Atmospheric Environment 111 (2015) 185–194

Contents lists available at ScienceDirect

Atmospheric Environment

journal homepage: www.elsevier.com/locate/atmosenv

Dynamic evaluation of air quality models over European regions

P. Thunis [a], E. Pisoni [a, *], B. Degraeuwe [a], R. Kranenburg [b], M. Schaap [b], A. Clappier [c]

[a] European Commission, JRC, Institute for Environment and Sustainability, Air and Climate Unit, Via E. Fermi 2749, Ispra, 21027 VA, Italy
[b] TNO, Department Climate, Air and Sustainability, P.O.Box 80015, 3508 TA Utrecht, The Netherlands
[c] Université de Strasbourg, Laboratoire Image Ville Environnement, 3, rue de l'Argonne, 67000 Strasbourg, France

HIGHLIGHTS

- Air quality model responses to emission reduction scenarios are presented.
- Maximum potential for local emission abatement is identified.
- Relative importance of the various precursor emissions is assessed.
- Degree of non-linearity of the model responses is estimated.
- Three case studies in Europe are considered.

ARTICLE INFO

Article history:
Received 17 December 2014
Received in revised form
7 April 2015
Accepted 8 April 2015
Available online 9 April 2015

Keywords:
Potency indicators
Air quality planning
Emission reductions
Non-linearity

ABSTRACT

Chemistry-transport models are increasingly used in Europe for estimating air quality or forecasting changes in pollution levels. But with this increased use of modeling arises the need of harmonizing the methodologies to determine the quality of air quality model applications. This is complex for planning applications, i.e. when models are used to assess the impact of realistic or virtual emission scenarios. In this work, the methodology based on the calculation of potencies proposed by Thunis and Clappier (2014) to analyze the model responses to emission reductions is applied on three different domains in Europe (Po valley, Southern Poland and Flanders). This methodology is further elaborated to facilitate the inter-comparison process and bring in a single diagram the possibility of differentiating long-term from short-term effects. This methodology is designed for model users to interpret their model results but also for policy-makers to help them defining intervention priorities. The methodology is applied to both daily PM_{10} and 8 h daily maximum ozone.

1. Introduction

Air quality models are increasingly used in Europe for simulating air quality. In the past, assessment and reporting of air quality was largely based on monitoring data but the situation has changed in recent years when more emphasis has been put on the use of air quality models to complement monitoring data. This is the result, among others, of the 2008 European Directive on Ambient Air Quality and Cleaner Air for Europe which encourages modeling as one of the means to perform AQ management tasks such as air quality assessment, forecasting and planning (EEA, 2011). With increasing number of air quality modeling applications, the need of harmonizing the methodologies to check the quality of air quality model applications is high. It is in this context that validation protocols are currently being developed in the frame of the Forum for Air Quality Modeling – FAIRMODE initiative (see http://fairmode.jrc.ec.europa.eu/). Since air quality models can be used to perform various tasks (assessment, forecasting, planning) specific validation protocols (i.e. Dennis et al., 2010, i.e. for assessment) should be developed and used.

Regarding assessment (or operational model evaluation, i.e. the reconstruction of past/present pollution episodes) the validation procedure usually makes use of real measurement at monitoring stations, that allows quantifying the quality of a given model simulation. In this context various protocols/tools have already been developed (e.g., Delta Tool, http://aqm.jrc.ec.europa.eu/DELTA/, see Thunis et al., 2012; Carnevale et al., 2014; Dennis et al., 2010; etc.)

Regarding forecasting (i.e. the application of a model to foresee

* Corresponding author.
E-mail address: enrico.pisoni@jrc.ec.europa.eu (E. Pisoni).

http://dx.doi.org/10.1016/j.atmosenv.2015.04.016

short-term pollution concentrations, see i.e. Aguilera et al., 2013), measurement can also be used to assess model performances. Specific indicators can then be used. We refer to Zhang et al. (2012) for an interesting overview of possible validation approaches.

The situation is more complex (and challenging) for planning applications, i.e. when models are used to assess the impact of realistic or virtual emission changes (Lefebvre et al., 2011). The FAIRMODE guidance document (EEA, 2011) reviews some possible methodologies to achieve this evaluation task:

(1) Trends analysis (i.e. the reproduction of two (or more) years characterized by change of emissions). Although this provides valuable information on the model capability to react properly to emission changes, the main disadvantage is to mix various factors in the analysis, in particular meteorology and emissions. In addition, the emission change across years remains affected by uncertainty (Fagerli and Aas, 2008).
(2) Time segregation. With this methodology a split of a long time period in smaller clusters (week-end vs. week days, day vs. night, summer vs. winter, etc.) is performed. Each of these clusters is characterized by different emissive characteristics (e.g., traffic emissions would mostly occur during week-days and decrease substantially on week-ends). By splitting data into clusters, meteorological conditions are mostly filtered out and the impact of emission changes can then be more easily identified.

Note that both of these two methodologies rely on the availability of measurement data to test the dynamic response of the air quality models.

Complementary to these two approaches, a method to further pursue the planning evaluation process is based on model inter-comparison exercises. Although measurement data could also be used if this inter-comparison is combined with one of the two above mentioned approach, the inter-comparison can also focus on virtual emission scenarios for which no measurement data exists. No comparison with the "truth" can then be made but this type of exercise however proves to be extremely useful to better understand/flag out "strange" model behaviors (Cuvelier et al., 2007; Pernigotti et al., 2013; Giannouli et al., 2011).

In this work we apply and further develop the methodology proposed by Thunis and Clappier (2014) to illustrate to what extent this approach can support the evaluation of air quality models in planning mode, in the frame of an inter-comparison exercise. This methodology is based on indicators and diagrams that aim at synthetizing in a systematic manner the key aspects of air quality model responses to emission changes. These indicators aim at responding the following three questions:

(1) What is the concentration change related to an emission precursor reduction in a given geographical area (i.e. how much of the observed concentration levels is controllable from abatement actions taken within the domain of interest)?
(2) What is the ratio of the concentration change corresponding to the abated emissions of a given precursor with respect to the others?
(3) How robust are model responses to emission changes (i.e. assess the modeled concentration variability for different emission reduction levels)?

In this work the proposed indicators are applied on a series of geographical areas (characterized by high levels of pollution) to illustrate their potential in terms of interpretation and inter-comparison. Results for both daily averaged PM_{10} and daily 8 h maximum O_3 are presented.

Section 2 provides a description of the modeling set-up; Section 3 describes the methodological aspects whereas Section 4 includes the discussion of the results. Conclusions are presented in Section 5.

2. Modeling set-up

For the current work, simulations were performed with the chemistry transport model LOTOS-EUROS (Hendriks et al., 2013; Beltman et al., 2013; Manders et al., 2009). Gas-phase chemistry is simulated using the TNO CBM-IV scheme, which is a condensed version of the original scheme (Whitten et al., 1980). Hydrolysis of N_2O_5 is explicitly described following Schaap et al. (2004). LOTOS-EUROS explicitly accounts for cloud chemistry computing sulphate formation as a function of cloud liquid water content and cloud droplet pH as described in Banzhaf et al. (2012). For Aerosol chemistry LOTOS-EUROS features the thermodynamic equilibrium module ISORROPIA2 (Fountoukis and Nenes, 2007). Dry Deposition fluxes are calculated following a resistance approach as described in Erisman et al. (1994). Furthermore, a compensation point approach for ammonia is included in the dry deposition module (Wichink Kruit et al., 2012).

LOTOS-EUROS was applied over three different geographical areas in Europe (Benelux, South of Poland and Po Valley, Fig. 1) with a spatial resolution of 7×7 km^2. In these three domains, the emissions have then been reduced in a specific sub-area of the domain (indicated by the dark grey shaded areas in Fig. 1: Flanders, Silesia and Lombardy, respectively) while emissions outside these areas are kept at base-case level for all scenarios. This simulation setting is motivated by the objective of analyzing regional/local emission reduction measures to be implemented on-top of the EU-wide measures.

Following the methodology proposed by Thunis and Clappier (2014) (see next section for a brief description and publication for more details) a series of independent simulations in which the emissions of the different precursors are reduced either independently or contemporarily is requested. For two levels of emission reductions, the number of simulations is equal to $2^*n + 3$ where n is the number of emission precursors to be tested. In the case of PM10 which depends on emissions from the NO_x, SO_2, NH_3, Primary Particulate Matter (PPM) and Volatile Organic Carbon (VOC) precursors, the number of simulations requested to calculate the indicators is 12 in addition to the base case. These simulations consist of:

- A base case simulation.
- Five simulations where each precursor is abated by 50%. It represents a compromise between a large enough reduction to capture the main aspects of the model responses to significant changes in the input data and a level of reduction which remains realistically achievable in terms of human activity constraints.
- Five simulations where each precursor is abated by 20%. These simulations are used to calculate the indicators with a second level of reduction and test the robustness of the model responses.
- Two simulations in which all 5 precursor emissions are reduced contemporarily by 20 and 50%, respectively. These simulations are used to assess the degree of non-linearity in model responses.

For O_3 the number of runs may be reduced to 6 sensitivity simulations in addition to the base case since O_3 formation depends mainly on two precursors: NO_x and VOC. However, all simulations requested for O_3 are already covered with those performed for PM_{10}.

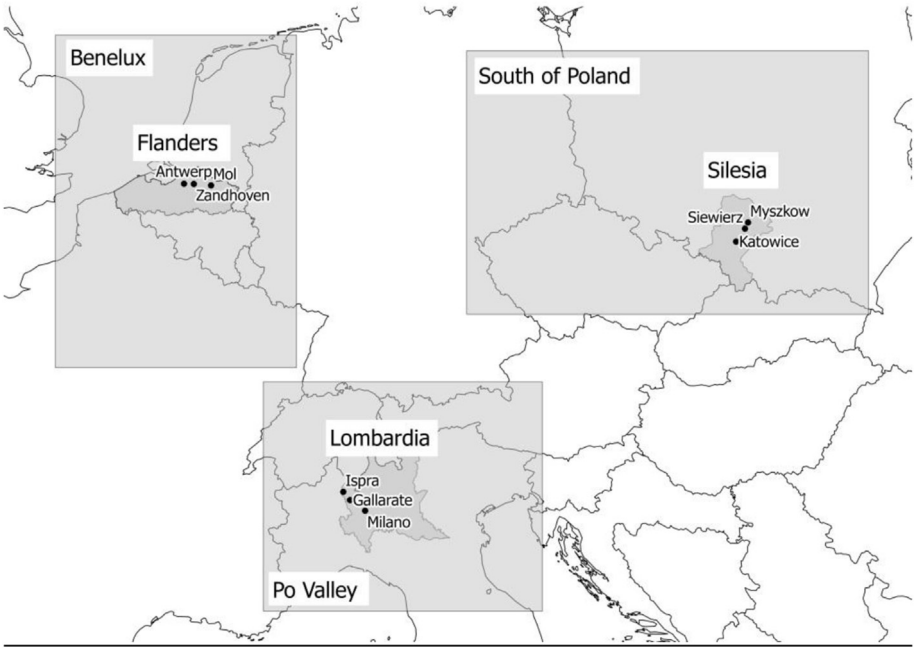

Fig. 1. Map of the three simulated areas (Benelux, South of Poland and the Po Valley). In this Figure, "light gray" represents the simulation domains, while "dark grey" the regional areas for which emissions have been reduced.

3. Methodological overview

In this section we recall briefly the main elements of the Thunis and Clappier (2014) methodology (for more details the reader is referred to the full publication) which propose indicators to deliver information about the effect of emission reductions on concentrations.

3.1. Potencies and indicators

A relative potency "p" (i.e. a relative concentration change resulting from a relative emission change) is defined for each of the twelve scenarios previously described, as follows:

$$p_\alpha^k = \frac{\Delta C_\alpha^k}{\alpha C}; p_\alpha^{ALL} = \frac{\Delta C_\alpha^{ALL}}{\alpha C} \quad (1)$$

Where α is the emission reduction level (20 or 50%), "k" is the selected precursor ("ALL" stands for the scenario in which all precursors are reduced contemporarily), C is the base case concentration level and $\Delta C_\alpha^k = C_\alpha^k - C$ $(\Delta C_\alpha^{ALL} = C_\alpha^{ALL} - C)$ is the concentration change between the base case and the emission reduction scenario concentrationC_α^k (C_α^{ALL}).

Based on these relative potencies two indicators are defined to construct the potency diagram. The first indicator (I^{max}, x-axis) is the maximum potency which provides the maximum concentration change resulting from an emission reduction. This maximum impact might result from either a combined reduction of all precursors or through the reduction of one single precursor if different precursors lead to opposite impacts and tend to counter-balance each other. I^{max} is therefore equal to the maximum (in absolute values) among p_α^{ALL} and the series of individual p_α^k.

In general, I^{max} is equal to p_α^{ALL} but it can occasionally be equal to one of thep_α^k if the effect of reducing one precursor alone is more important than the effect of the simultaneous reduction of all precursors.

I^{max} can reach 0 meaning that emission reductions have no impact on the concentrations levels observed within the domain of interest (background impacts strongly dominates), be close to −1 when emission reductions are fully effective and reduce concentration levels in the same proportion as emission reductions but can also be positive when overall emission reductions lead to a concentration increase.

The second indicator (J_α^k , y-axis) provides information on the importance of a given single precursor impact in terms of concentration change relatively to the others. It is formulated as:

$$J_\alpha^k = \frac{I_\alpha^k}{|I^{\max}|} \quad (2)$$

This indicator ranges between 0 (no impact) and −1 (the single precursor is responsible for the entirety of the impact) with positive values indicating concentration increases resulting from the given precursor emission decrease.

I^{max} and J_α^k are calculated for each grid cell within the domain for the reference emission reduction level (i.e. 50%) and plotted in the potency diagram. The operation is then repeated for the intermediate reduction level (20%) and lines are drawn between each of the 50% point and the location that would be obtained with 20%. This line provides a quantitative estimate of the robustness or in other terms the degree of variation of the model response when different levels of reductions are applied. This information is key for policy makers to ensure that a decision is not too sensitive to input parameters.

Through diagrams and maps (as shown in the next Sections) it is then possible to visualize the aforementioned indicators, to allow for air quality model evaluations in the context of decision making.

4. Results

Based on the 13 LOTOS-EUROS air quality simulations, the indicators defined in Section 2 can be computed and the diagrams constructed for each geographical area and precursor. A complete interpretation is first provided for one specific region, i.e. considering PM_{10} for the Benelux, in terms of a) maximum potency and precursor contributions, and b) robustness. We then introduce

some assumptions to summarize these diagrams in order to inter-compare the results obtained for all the three considered case studies.

4.1. Application of the "potency diagram" over the Benelux region

Fig. 2 depicts the PM_{10} potency diagrams for the Benelux domain. The five diagrams correspond to each of the 5 precursors (NO_x, VOC, NH_3, SO_2 and PPM), with each point being one domain grid-cell value. As mentioned above, the maximum potency (I^{max}, x-axis) represents the maximum impact that can be obtained from reducing local (regional) emissions and is therefore equal in all diagrams for a given region. In the case of Flanders it reaches roughly 30%, meaning that an emission reduction of 50% would lead to a concentration decrease of roughly 16% (or similarly a concentration decrease of 30% when emissions are dropped to zero, if linearity is assumed). This also implies that air quality improvements beyond these 30% should be searched through "beyond-regional" emission control measures (i.e. national or European) as only 30% of improvement can be managed through regional emission reductions.

The y-axis provides information on the impact of a given precursor in comparison to the other precursors. It is clear that NH_3 and PPM are the two most impacting precursors in this study area, while NO_x, SO_2 and VOC have all a limited local impact.

Multiplying the two indicators $I^{\max}$ and J^k_α leads to I^k_α which provides information on the percentage impact of the considered precursor on concentrations. This information is given by the hyperbolas which represent precursor impacts of 10%, 25% and 50%, respectively starting from the origin point outwards. The impact on concentrations is generally lower than 10% with the only exception of PPM. The colors in the Figures (blue, green and red (in the web version)) represent respectively the 20, 80 and remaining (100%) concentration percentiles and are used to underline potency behaviors related to different concentrations levels.

While Fig. 2 shows information on the maximum precursor impact for the Benelux area (i.e. local vs. boundary impact) and on precursor contributions (precursor vs. precursor impact and precursor impact on concentrations) no spatial information is provided by this type of diagrams. In Fig. 3 the maximum impact $I^{\max}$ is spatially represented, showing a higher potential impact in the central part of the emission reduction area, i.e. the agglomerations of Brussels and Antwerp.

To analyze the robustness of the model responses, the scenarios performed with 20% emission reductions are used to re-calculate the indicators. As mentioned in the previous section a line can be drawn to represent robustness. These lines are not shown here as they are small and therefore not visible. In addition they appear only for small concentration values pointing out to the high robustness obtained for yearly averaged PM_{10} concentrations.

4.2. Inter-comparison of model responses across geographical areas

For the scope of the inter-comparison among different regions we first simplify the approach by focusing only on model responses for the highest concentration percentile, as this is the range of concentration where improvement is generally of interest. This is an arbitrary choice, but it is not affecting the proposed procedure to analyze model responses to emission reductions. We also try to differentiate model responses between long-term average and short-term episodic concentrations. The approach which is performed for the daily average PM_{10} and the 8 h daily maximum O_3 relies on the indicator previously described. Within each geographical emission-reduction area, we operate as follows:

1) Selection of the grid cells with the highest yearly (PM_{10}) or summer (O_3) averaged concentrations. This can be a percentile or a number of cells exceeding a desired threshold. In our case we arbitrarily selected the 10 grid cells with the highest value

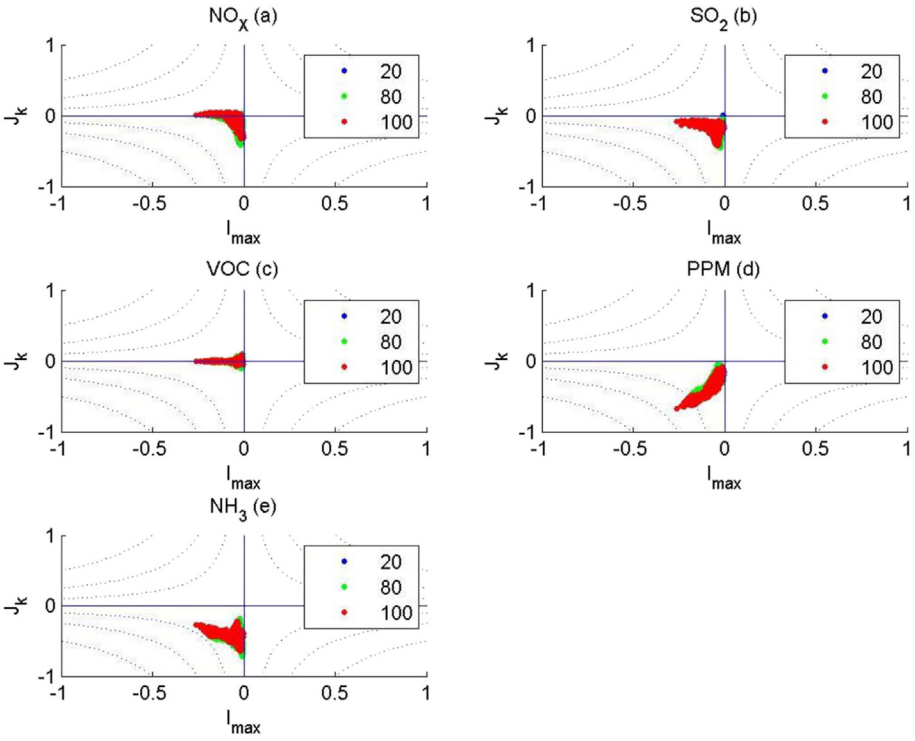

Fig. 2. Indicator diagram for the Benelux domain, at 7 × 7 km^2 resolution, applying 20% reductions, for PM_{10} concentrations, considering emission reductions for NO_x (a), SO_2 (b), VOC (c), PPM (d) and NH_3 (e).

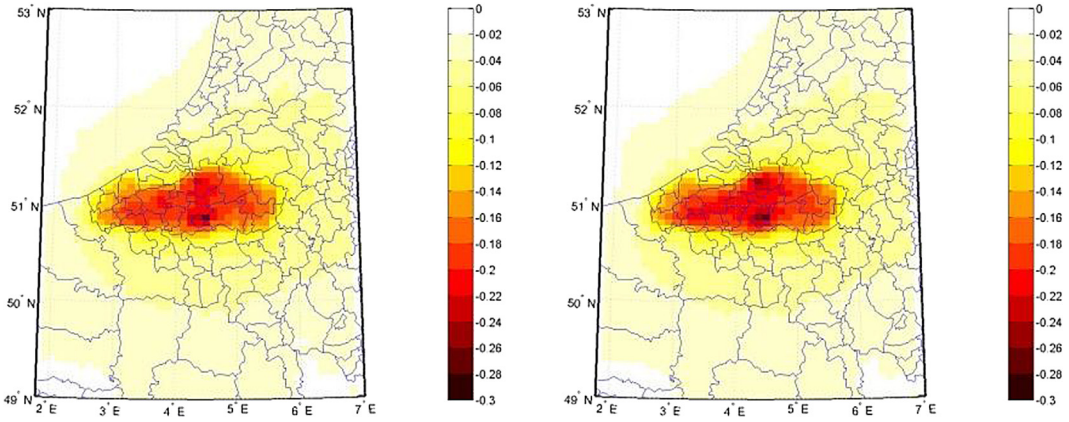

Fig. 3. Map showing the maximum (across the simulated scenarios) potency for the Benelux domain, at 7 × 7 km^2 resolution, for PM_{10} concentrations, applying 20% (left) and 50% (right) emission reductions.

within the emission reduction domain, to focus on the improvement one can reach in the worst case.
2) For each of these 10 grid cells, calculation of p_α^k and p_α^{ALL} for each precursor "k" and for the two levels of emission reduction (20 and 50%). For each grid cell we define then the maximum, minimum and mean value for each of these indicators.
3) For the grid cells showing the highest concentration value, we extract the time series (year for PM_{10} and summer for O_3) and similarly to what has been done spatially (step 1 & 2), we arbitrarily only keep the highest concentration values, in our case the 10 highest.
4) For each of these 10 concentrations identified in the time series, we calculate the maximum, minimum and mean potencies, to simplify the visualization phase.

Fig. 4 illustrates graphically the result of this approach for PM_{10} over the Benelux. The diagram is organized as follows:

1) Potencies for each precursor (NO_x, VOC, NH_3, PPM and SO_2) are expressed along a specific rectangle. Within each of these rectangles, the dark (light) blue lines links the minimum and maximum potencies obtained with 50% (20%) for the long-term concentration averages while the circle represents the average potency. The red and orange lines follow the same principle but for the highest episodic concentrations.
2) The last rectangle provides information about non-linearity. It results from the difference between the sum of all individual potencies and the "all together potency, i.e. $Int = \sum p_\alpha^k - p_\alpha^{ALL}$(see Equation (1) for details on the two terms).

We see from Fig. 4 that long-term averaged model responses are mostly dominated by PPM and NH_3 while local reductions in other precursors are almost not efficient. The responses are very robust (the circles and lines obtained with 20% and 50% coincide) and that the degree of non-linearity is almost negligible (bottom rectangle). This result is also confirmed by a previous study (Thunis et al., 2015). For episodic high values, the conclusions drawn in terms of robustness and non-linearity still hold but slightly larger potencies are modeled. Non-linearity becomes also slightly more important in some regions.

Similarly, Figs. 5–9 are constructed for the two other regions for daily PM_{10} and the 8 h daily maximum O_3. We note the following points for PM_{10}.

1) For PM_{10} combined precursor reductions always lead to maximum impacts which are of the order of 50% over the Poland and Po Valley area but restricted to about 30% in the Benelux.
2) For both long-term and episodic responses, the dominating precursor is PPM in all regions followed by NH_3. Other precursors have impacts but they are region specific (e.g., NO_x and SO_2 in Lombardy)
3) The responses for episodic events follow the same general trends but tend to reach higher potencies indicating the larger control a region can have on abating episodic values rather than long term averaged ones. This is especially true in the South of Poland domain.
4) All model responses (long-term and episodic) are generally very robust (i.e. the circles and lines do overlay) and weakly non-linear (low values reached in the last rectangle)
5) It is interesting to note that in the Benelux domain the potencies for episodic events are lower than those associated to long-term averages, indicating a potentially larger (than in average conditions) import from the outside the reduction area during high concentration episodes.

For the daily 8 h max O_3 we note that:

1) The impact on summer averaged values is very modest in all regions while the impact on episodic values becomes more important in some regions like the Po Valley where it reaches 0.25.
2) As expected the responses to other precursors than NO_x and VOC are negligible. Significant responses to NO_x are only seen in the Po-Valley
3) Similarly to PM_{10}, the robustness of the long-term averaged responses is quite good but it tends to be weaker for episodic responses (e.g., NO_x in the Po-Valley). The same observation holds for the interaction term which becomes important for episodic events in some regions.

Figs. 10 and 11 show the interaction (Int) component for PM_{10} and O_3 respectively obtained with a 50% emission reduction in terms of the concentration percentiles, from lowest to highest. It can be seen that the maximum value of this non-linear component does not occur for the highest percentiles, explaining the low values generally found in our analysis.

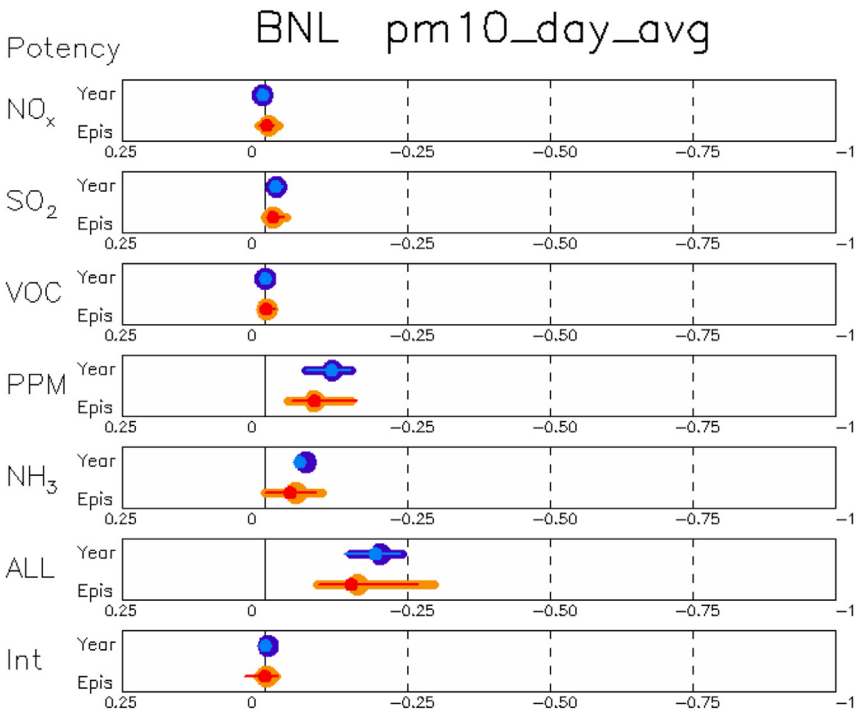

Fig. 4. Summary PM_{10} Potency diagram for the Benelux region (emissions reduced over Flanders). See text for explanations.

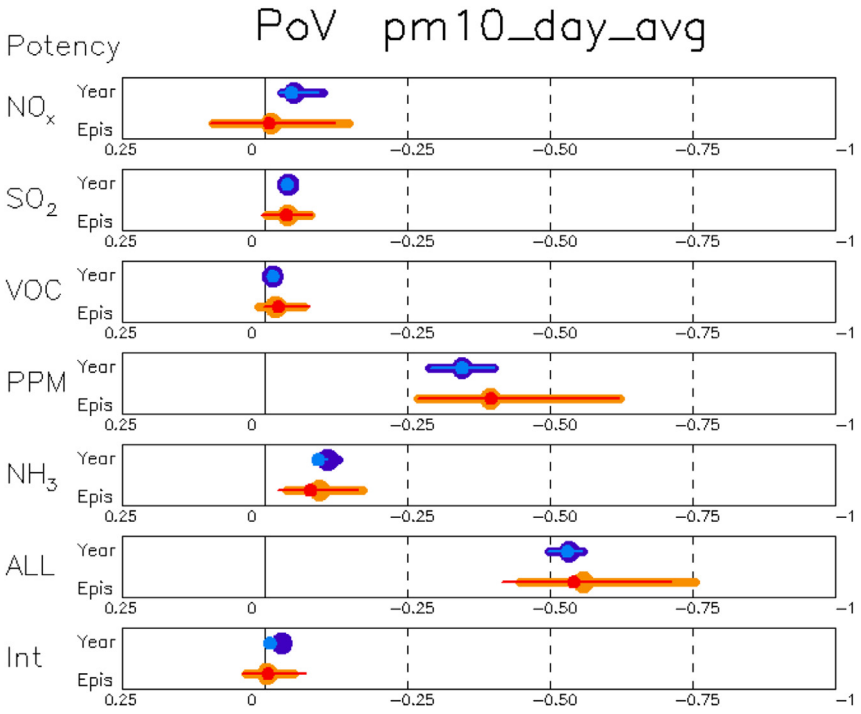

Fig. 5. Summary PM_{10} Potency diagram for the Po-Valley region (emissions reduced over Lombardy). See text for explanations.

4.3. Comparison with other studies

Although many publications address the issue of evaluating the impact of emission reduction scenarios on air quality, the results are generally not reported in a harmonized way. It is therefore difficult to make comparisons among this paper and previous works, with the exception of few cases in which similar assumptions to the one used in this paper are considered. For example de Meij et al. (2009) presented an "extreme case" simulation performed on the Lombardy region, in which regional emissions were brought down to 0, leading to a PM air quality improvement of 50% during an episode and therefore to a potency of 0.5 comparable to the "0.6 value" reported in this work. Similar responses have been found by Carnevale et al. (2010) who applied a

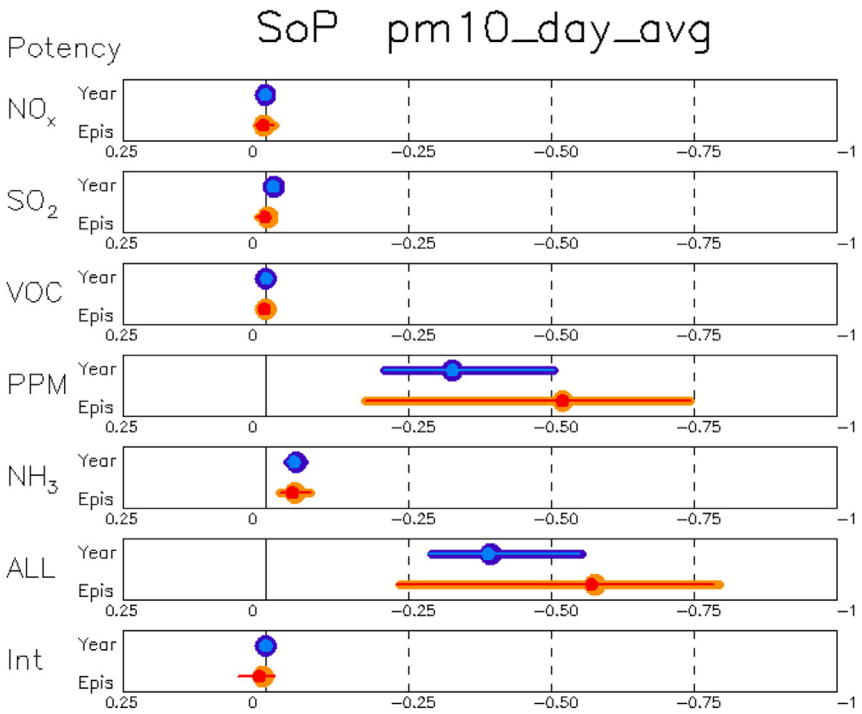

Fig. 6. Summary PM_{10} Potency diagram for the South Poland region (emissions reduced over Silesia). See text for explanations.

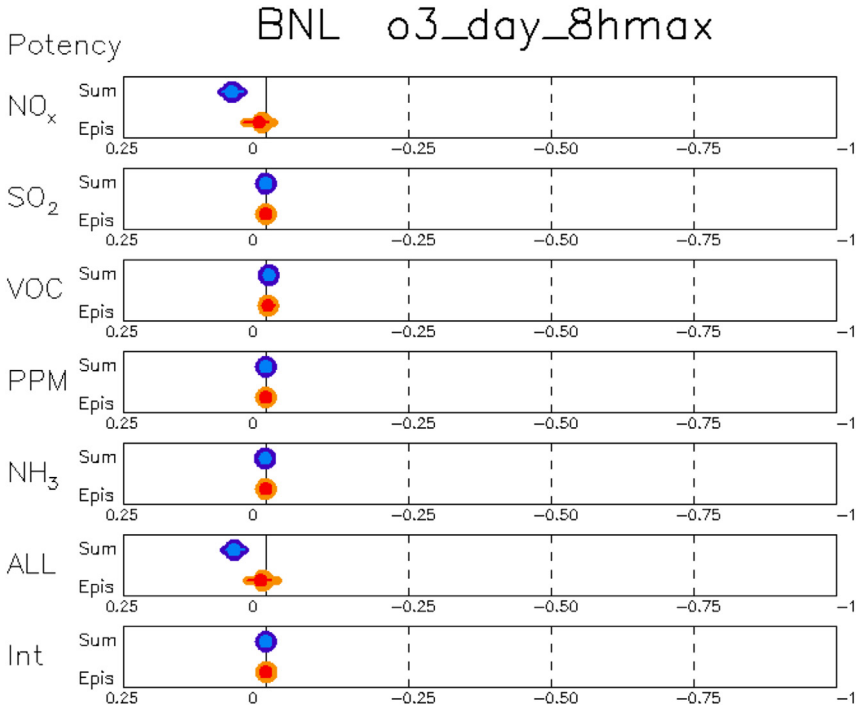

Fig. 7. Summary O_3 Potency diagram for the Benelux region (emissions reduced over Flanders). See text for explanations.

"factor separation analysis" leading to potency values between 0.5 and 0.6. Korsholm et al. (2012) simulated the effects of building insulation on ground-level air pollutants concentration levels over Western Europe (applying EU level reductions) and found PM_{10} concentration reduction by 3.6% for a 9% PPM emission reduction (again, in line with the results obtained for the Po Valley and Benelux in this paper). Andreani-Aksoyoğlu et al. (2008) simulated the effect of a complete elimination of anthropogenic emissions in Switzerland on O_3 concentrations and found that ozone level would drop down by 5% (in line with the results obtained in this paper). Banzhaf et al. (2013) showed that non-linearities in the "emission to concentration" link should be accounted for episodes characterized by high secondary inorganic aerosol concentrations. Their tests considered NH_3 emission reductions applied on both Germany

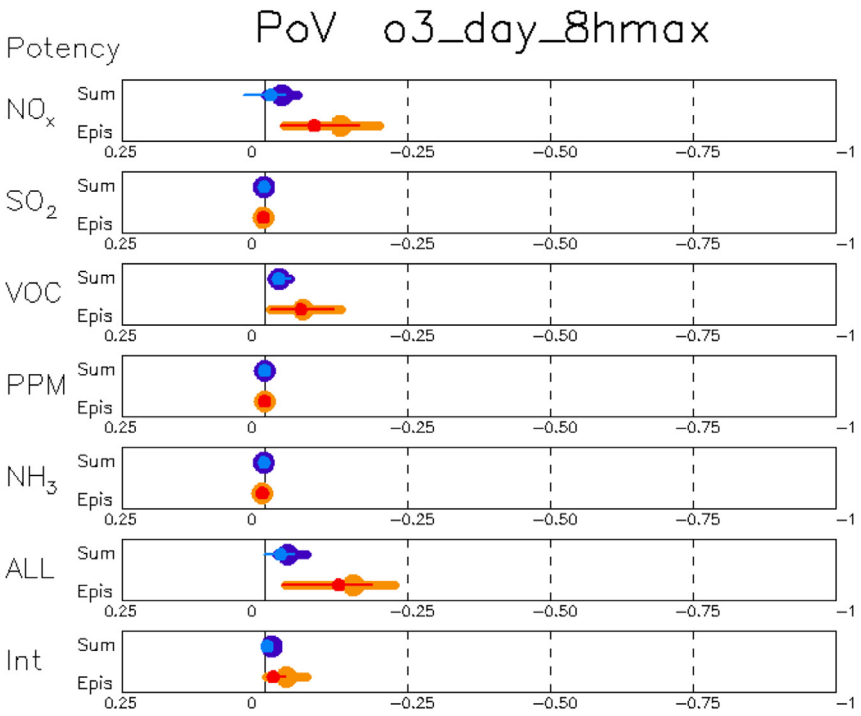

Fig. 8. Summary O_3 Potency diagram for the Po-Valley region (emissions reduced over Lombardy). See text for explanations.

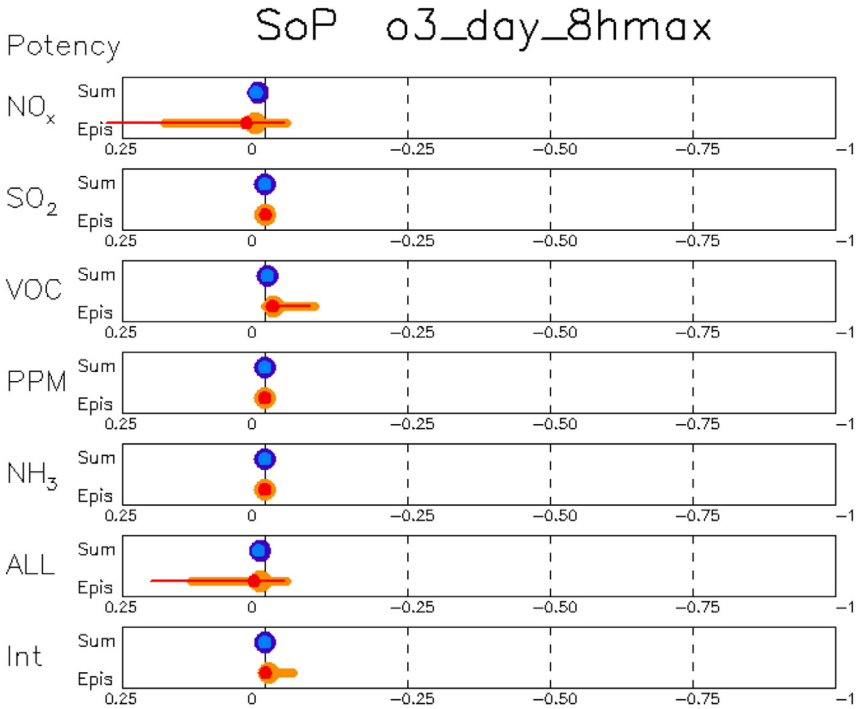

Fig. 9. Summary O_3 Potency diagram for the South Poland region (emissions reduced over Silesia). See text for explanations.

and the entire European domain. Bessagnet et al. (2014) also performed simulations to analyze model sensitivity to NH_3 emission reductions with three models (CHIMERE, EMEP and LOTOS-EUROS) and for three different emission reduction scenarios (10%, 20% and 30%). Their results showed that the impact of NH_3 emission reductions on the number of station in exceedance of the daily limit value was non-linear, while the impact on yearly averaged values was closer to linear.

Despite their quantitative aspect, these comparisons remain qualitative since the set-up of each of these referenced works differs in terms of air quality model used, domain extension, etc. One of the main advantages of the approach presented in this paper is to deliver a dimensionless summary of the model responses, which can easily be used to inter-compare models or domains among each other's.

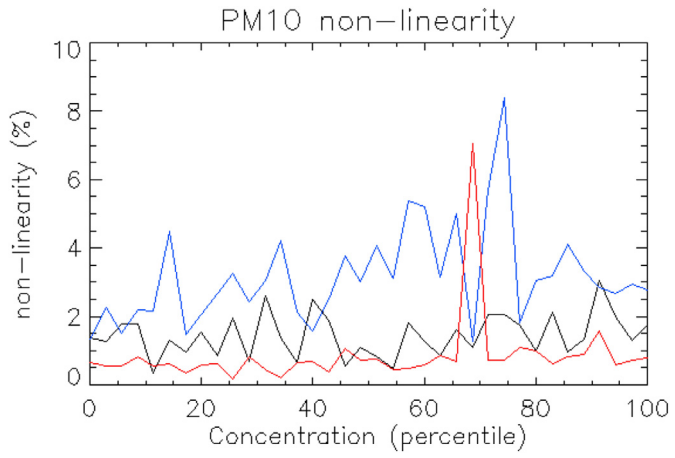

Fig. 10. Average non-linearities for daily PM_{10} in terms of concentrations organized in percentiles (from low to high concentrations). Concentrations are sorted and clustered in groups of 10 values based on which an average non-linearity is calculated. The three domain are represented with different colors, with Flanders in black, Lombardy in blue and Silesia in red. (For interpretation of the references to color in this figure legend, the reader is referred to the web version of this article.)

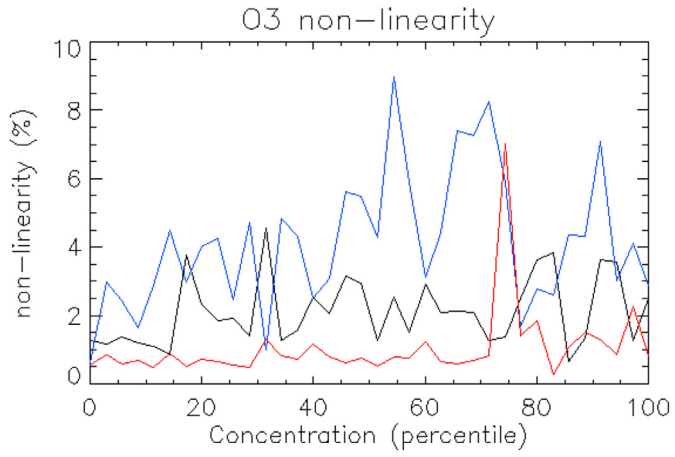

Fig. 11. Same as Fig. 10, but for the 8 h daily maximum O_3.

5. Conclusions

In this work, the methodology based on the calculation of potencies proposed by Thunis and Clappier (2014) to analyze the model responses to emission reductions is applied on three different domains in Europe. This methodology is further elaborated to facilitate the inter-comparison process and bring in a single diagram the possibility of differentiating long-term from short-term effects. This methodology is designed for model users to interpret model results on air quality planning and help policy-makers in prioritizing policies.

Based on a set of 12 emission reduction scenario simulations performed with LOTOS-EUROS (in addition to a base-case simulation) potency indicators are calculated, which can be used for the following purposes:

- Identifying the potential of local emission abatement action vs. transport across the domain boundary;
- Assessing the relative importance of the various precursors emission which have a potential impact on concentrations;
- Estimating the robustness of the model responses (i.e., how much would my response change if another reduction level is selected?);
- Estimating the degree of non-linearity among precursors (i.e. how would my response change if I reduce all precursors contemporarily rather than sequentially?).

Application of the methodology over the three domains (Benelux, South Poland and Po Valley) has allowed answering the above questions. In particular this methodology revealed to be very useful to compare the responses across regions in a uniform way. Assessing quantitatively the importance of robustness and non-linearities can proof to be very useful also in terms of developing surrogate models for integrated assessment (IA). Indeed IA models make use of surrogate (simplified) models to mimic the reality with some degree of fidelity. The approach proposed here can serve this purpose by better understanding the model behavior and setting up priorities, i.e. by selecting between processes which need to be reproduced and those which can be neglected.

With a limited number of simulations (i.e. 12 simulations + a base-case simulation) a summary “status template” can be elaborated to support policy makers in their analysis of possible options (choice of local abatement measures to improve air quality, prioritization of potential interventions…) to abate air pollution in the most efficient way. Obviously this study remains domain and model dependent but the methodology applied here can be used as a basis for a common inter-comparison framework. Also, the assumptions used in this paper (as the fact that emission scenarios consider constant reductions, the choice of the number of cells/days to compute summarized potencies, the dimension of the emission reduction areas, etc…) will be further investigated in the near future, to test the robustness of the proposed approach.

Although the number of simulations required by the methodology is limited, the task remains substantial (in terms of computational burden) and only three areas could be covered in this work. Future work will consist in extending the approach to 1) other areas in Europe (e.g., southern countries) to assess model responses and their associated non-linearities in different environments and under different chemical regimes; 2) other modeling approaches and 3) to analyze model responses in terms of activity sectors (in addition to the precursor analysis proposed here) to better support policy makers in their decisions.

References

Aguilera, I., Basagaña, X., Pay, M.T., Agis, D., Bouso, L., Foraster, M., Rivera, M., Baldasano, J.M., Künzli, N., 2013. Evaluation of the CALIOPE air quality forecasting system for epidemiological research: the example of NO2 in the province of Girona (Spain). Atmos. Environ. 72, 134–141.

Andreani-Aksoyoğlu, S., Keller, J., Ordóñez, C., Tinguely, M., Schultz, M., Prévôt, A., 2008. Influence of various emission scenarios on ozone in Europe. Ecol. Model. 217, 209–218.

Banzhaf, S., Schaap, M., Kruit, R.J. Wichink, van der Gon, H.A.C. Denier, Stern, R., Builtjes, P.J.H., 2013. Impact of emission changes on secondary inorganic aerosol episodes across Germany. Atmos. Chem. Phys. 13, 11675–11693.

Banzhaf, S., Schaap, M., Kerschbaumer, A., Reimer, E., Stern, R., van der Swaluw, E., Builtjes, P., 2012. Implementation and evaluation of pH-dependent cloud chemistry and wet deposition in the chemical transport model REM-Calgrid. Atmos. Environ. 49, 378–390.

Beltman, J., Hendriks, C., Tum, M., Schaap, M., 2013. The impact of large scale biomass production on ozone air pollution in Europe. Atmos. Environ. 71, 352–363.

Bessagnet, B., et al., 2014. Can further mitigation of ammonia emissions reduce exceedances of particulate matter air quality standards? Environ. Sci. Policy 44, 149–163.

Carnevale, C., Pisoni, E., Volta, M., 2010. A non-linear analysis to detect the origin of PM10 concentrations in Northern Italy. Sci. total Environ. 409, 182–191.

Carnevale, C., Finzi, G., Pederzoli, A., Pisoni, E., Thunis, P., Turrini, E., Volta, M., 2014. Applying the delta tool to support the air quality Directive: evaluation of the TCAM chemical transport model. Air Qual. Atmos. Health 7, 335–346. http://dx.doi.org/10.1007/s11869-014-0240-4.

Cuvelier, C., et al., 2007. CityDelta: a model intercomparison study to explore the impact of emission reductions in European cities in 2010. Atmos. Environ. 41, 189–207.
de Meij, A., Thunis, P., Bessagnet, B., Cuvelier, C., 2009. The sensitivity of the CHIMERE model to emissions reduction scenarios on air quality in Northern Italy. Atmos. Environ. 43, 1897–1907.
Dennis, R., et al., 2010. A framework for evaluating regional-scale numerical photochemical modeling systems. Environ. Fluid Mech. 10, 471–489.
EEA, 2011. The Application of Models under the European Union's Air Quality Directive: a Technical Reference Guide. Technical report No 10/2011.
Erisman, J.W., van Pul, A., Wyers, P., 1994. Parametrization of surface-resistance for the quantification of atmospheric deposition of acidifying pollutants and ozone. Atmos. Environ. 28, 2595–2607.
Fagerli, H., Aas, W., 2008. Trends of nitrogen in air and precipitation: model results and observations at EMEP sites in Europe, 1980–2003. Environ. Pollut. 154 (3), 448–461.
Fountoukis, C., Nenes, A., 2007. ISORROPIAII: a computationally efficient thermodynamic equilibrium model for K+-Ca2+-Mg2+-NH4 +-Na+-SO4 2−NO3 −Cl-H2O aerosols. Atmos. Chem. Phys. 7 (17), 4639–4659.
Giannouli, G., Kalognomou, E., Mellios, G., Moussiopoulos, N., Samaras, Z., Fiala, J., 2011. Impact of European emission control strategies on urban and local air quality. Atmos. Environ. 45, 4753–4762.
Hendriks, C., Kranenburg, R., Kuenen, J., van Gijlswijk, P.P., Wichink Kruit, R.J., Segers, A.J., R. N., Denier van der Gon, H.A.C., Schaap, M., 2013. The origin of ambient particulate matter concentrations in the Netherlands. Atmos. Environ. 69, 289–303.
Korsholm, U.S., Amstrup, B., Boermans, T., Sørensen, J.H., Zhuang, S., 2012. Influence of building insulation on outdoor concentrations of regional air-pollutants. Atmos. Environ. 54, 393–399.
Lefebvre, W., Fierens, F., Trimpeneers, E., Janssen, S., Van de Vel, K., Deutsch, F., Viaene, P., Vankerkom, J., Dumont, G., Vanpoucke, C., Mensink, C., Peelaerts, W., Vliegen, J., 2011. Modeling the effects of a speed limit reduction on traffic-related elemental carbon (EC) concentrations and population exposure to EC. Atmos. Environ. 45, 197–207.
Manders, A.M.M., Schaap, M., Hoogerbrugge, R., 2009. Testing the capability of the chemistry transport model LOTOS-EUROS to forecast PM10 levels in the Netherlands. Atmos. Environ. 43, 4050–4059.
Pernigotti, D., et al., 2013. POMI: a model inter-comparison exercise over the Po Valley. Air Qual. Atmos. Health 6, 701–715.
Schaap, M., van Loon, M., ten Brink, H.M., Dentener, F.D., Builtjes, P.J.H., 2004. Secondary inorganic aerosol simulations for Europe with special attention to nitrate. Atmos. Chem. Phys. 4, 857–874.
Thunis, P., Clappier, A., Pisoni, E., Degraeuwe, B., 2015. Quantification of non-linearities as a function of time averaging in regional air quality modeling applications. Atmos. Environ. 103, 263–275.
Thunis, P., Clappier, A., 2014. Indicators to support the dynamic evaluation of air quality models. Atmos. Environ. 98, 402–409.
Thunis, P., Pederzoli, A., Pernigotti, D., 2012. Performance criteria to evaluate air quality modeling applications. Atmos. Environ. 59, 476–482.
Wichink Kruit, R.J., Schaap, M., Sauter, F.J., Van Zanten, M.C., Van Pul, W.A.J., 2012. Modeling the distribution of ammonia across europe including bi-directional surface-atmosphere exchange. Biogeosciences 9, 5261–5277.
Whitten, G., Hogo, H., Killus, J., 1980. The carbon bond mechanism for photochemical smog. Environ. Sci. Technol. 14, 14690–14700.
Zhang, Y., Bocquet, M., Mallet, V., Seigneur, C., Baklanov, A., 2012. Real-time air quality forecasting, part I: history, techniques, and current status. Atmos. Environ. 60, 632–655.